JOURNAL OF GUIDANCE, CONTROL, AND DYNAMICS
Vol. 21, No. 2, March–April 1998

Minimum-Time Maneuvers of Thrust-Vectored Aircraft

Arkadi Lichtsinder*
RAFAEL, Ministry of Defense, Haifa 31021, Israel
and
Eliezer Kreindler† and Benjamin Gal-Or‡
Technion—Israel Institute of Technology, Haifa 32000, Israel

The new aircraft technology of thrust vectoring (TV) enables the execution of new types of poststall maneuvers. Aircraft agility and flight safety are greatly enhanced. The objective and main contribution of the present work are the suboptimal solution of minimum-time pitch-reversal (there and back) and yaw-reversal standard agility comparison maneuvers (SACOM). It is demonstrated that, due to asymmetric and coupling moments at high α and high β, pure pitch and yaw maneuvers are impossible; a full six-degree-of-freedom model must be employed. A novel parametric two-stage suboptimization algorithm was developed to cope with the complexity of the optimal control problem. All four aerodynamic and three TV controls are simultaneously active in the execution of a low *g* load, nearly pure 80-deg pitch-reversal and a 30-deg yaw-reversal SACOM of an F-15B aircraft.

Nomenclature

b = reference span
C_D = drag coefficient
C_{fg} = thrust coefficient
C_L = lift coefficient
C_l = rolling moment coefficient
C_{lp} = roll damping derivative
C_{lr} = roll moment derivative with respect to yaw rate
$C_{l\beta}$ = roll moment derivative with respect to sideslip angle
$C_{l\delta a}$ = aileron effectiveness derivative
$C_{l\delta e}$ = elevator effectiveness derivative
$C_{l\delta r}$ = rudder effectiveness derivative
$C_{l\delta\Delta e}$ = differential elevator effectiveness derivative
C_m = pitching moment coefficient
C_{mo} = basic pitching moment coefficient
C_{mq} = pitching moment derivative with respect to pitch rate
C_n = yawing moment coefficient
C_{no} = basic yawing moment coefficient
C_{np} = yawing moment derivative with respect to yaw rate
C_{nr} = yawing damping derivative
$C_{n\beta}$ = yawing moment derivative with respect to sideslip angle
$C_{n\beta^*}$ = asymmetric yawing moment increment
$C_{n\delta a}$ = yawing moment derivative with respect to aileron deflection
$C_{n\delta e}$ = yawing moment derivative with respect to elevator deflection
$C_{n\delta r}$ = rudder effectiveness derivative
$C_{n\Delta\delta e}$ = yawing moment derivative with respect to differential stabilizator deflection
C_x = longitudinal force coefficient
C_y = side-force coefficient
C_{yp} = side-force derivative with respect to roll rate
C_{yr} = side-force derivative with respect to yaw rate
$C_{y\beta}$ = side-force derivative with respect to sideslip angle
$C_{y\beta^*}$ = asymmetric side-force increment
$C_{y\delta a}$ = side-force derivative with respect to aileron deflection
$C_{y\delta e}$ = side-force derivative with respect to elevator deflection
$C_{y\Delta\delta e}$ = side-force derivative with respect to differential stabilizator deflection
c = reference mean aerodynamic chord
h = altitude
I_x = moment of inertia about the roll axis
I_{xy} = cross product of inertia between roll and pitch axes
I_{xz} = cross product of inertia between roll and yaw axes
I_y = moment of inertia about the pitch axis
I_z = moment of inertia about the yaw axis
K_φ = banking-error weight coefficient
K_ψ = heading-error weight coefficient
l_x = distance from nozzle exit to aircraft center of gravity
l_y = distance between nozzle exit center and aircraft vertical centerplane
M = vehicle mass
N_{pr} = nozzle pressure ratio
p = roll rate
q = pitch rate
$\bar{q}$ = dynamic pressure, $\frac{1}{2}\rho V^2$
r = yaw rate
$\mathcal{S}$ = switching function
s = reference surface area
T_i = ideal isentropic (net) thrust
$T_{x,y,z}$ = thrust-vectored components in the body axis
t = time
t_f = final time
t_s = switching time
V = true airspeed
α = angle of attack
β = angle of sideslip
ΔC_l = roll moment increment due to two-place canopy
ΔC_n = yawing moment increment due to two-place canopy
$\Delta\delta_z$ = effective differential (roll) thrust-vectoring angle
δ = control vector
δ_a = aileron surface deflection
δ_e = elevator (stabilizator) surface deflection
δ_r = rudder surface deflection
δ_y = effective yaw thrust-vectoring angle
δ_z = effective pitch thrust-vectoring angle
$\delta_{\Delta e}$ = differential elevator surface deflection
θ = pitch angle
ρ = air density
φ = bank angle
ψ = heading angle

Received Dec. 26, 1996; revision received Aug. 14, 1997; accepted for publication Aug. 15, 1997.

*Research Engineer, Department of Platforms and Launchers, Department 42, P.O. Box 2250.
†Associate Professor, Department of Electrical Engineering, Technion City.
‡Professor and Head of Gas-Turbine and Jet Engines Laboratory, Department of Aerospace Engineering, Technion City.

I. Introduction

THE past decade witnessed rapid advances in the technology of thrust vectoring (TV) for aircraft.[1–3] The response time of

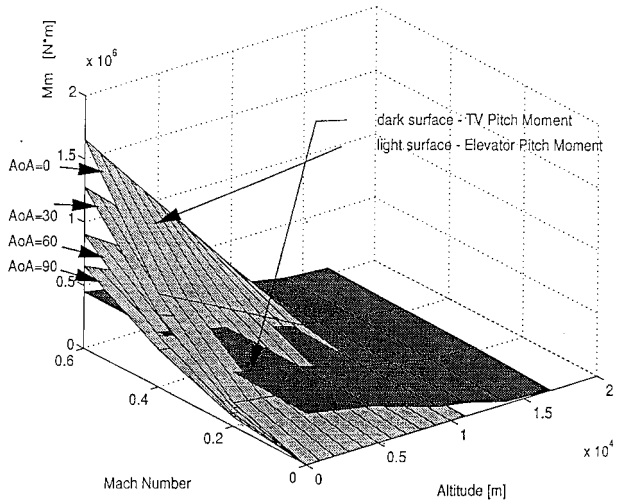

Fig. 1 Elevator vis-à-vis pitch TV comparison at δ_e and $\delta_z = -30$ deg.

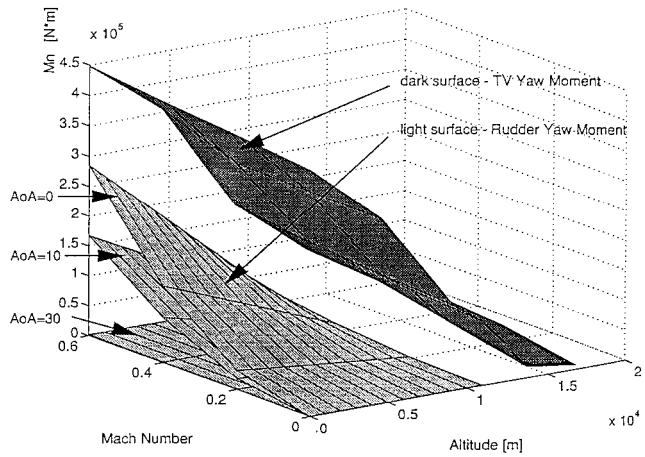

Fig. 2 Rudder vis-à-vis yaw TV comparison at δ_r and $\delta_y = 30$ deg.

thrust-vectoring controls is now comparable to that of the conventional aerodynamic controls, so that the former can complement or supersede the latter. In this technology, the jet stream is deflected by paddles and special nozzles.

Because TV is nearly independent of the airflow, its effectiveness vis-à-vis aerodynamic controls is most pronounced during high-angle-of-attack (high-α) flights and low-speed situations. This is seen in Figs. 1 and 2, where the pitch and yaw moments of TV and aerodynamic controls are compared for the F-15B.

The high-α capability of the TV aircraft enables it to execute new types of maneuvers, which vastly enhances its agility; dramatic advantages in close-range air combat were demonstrated in mock dogfights, e.g., a 32:1 kill ratio of a TV-equipped X-31 against a conventional F-18 (Ref. 4). Additional benefits of TV include the possibility of a reduced tail,[5] thereby reducing drag, weight, and observability. The potential benefits to flight safety are also being investigated.[6–8]

Full yaw-roll-pitch TV flight control capability was first demonstrated in 1987, by the Jet Laboratory, Technion—Israel Institute of Technology, flying powered subscale prototypes.[9] Currently, a number of full or partial TV-equipped, full-scale fighter aircraft prototypes are being flight tested.

The work reported here is in the context of standard agility comparison maneuvers (SACOM),[10,11] elementary maneuvers important for specification and assessment of fighter aircraft performance. The motivation for introducing these maneuvers as elements of aircraft agility—an involved topic—is discussed and referenced in Refs. 10 and 11. Of the seven basic SACOM proposed,[11] we consider maneuvers related to SACOM 2 and 3, namely, minimum-time pure pitch and yaw reversals for an F-15B aircraft. Specifically, a pure, minimum-time pitch reversal SACOM is one where the pitch angle θ and angular rate $\dot{\theta}$ undergo the change

$$[\theta(0) = 0, \dot{\theta}(0) = 0] \rightarrow \left[\theta\left(t_{f_1}\right) = \theta_f, \dot{\theta}\left(t_{f_1}\right) = 0\right]$$
$$\rightarrow \left[\theta\left(t_{f_2}\right) = 0, \dot{\theta}\left(t_{f_2}\right) = 0\right]$$

purely in the vertical plane and in minimum time t_{f_2}. The first phase, to θ_f, will be called to target, and the second phase back to $\theta = 0$ will be called the recovery. The minimum-time pure yaw reversal SACOM is similarly defined. Although fast fuselage is of tactical importance, the maneuvers we consider are elementary ones for comparison purposes. Because of asymmetric forebody vortices, a pure maneuver is shown in Sec. II to be impossible; this is even more so for a pure yaw reversal, similarly defined, where strong roll-yaw coupling at high α and β must be taken into account. We therefore employed a fairly complete six-degree-of-freedom simulation model for the F-15B, described in Sec. III. Because of the complexity of the model, a novel two-stage suboptimal algorithm, presented in Sec. IV, was developed. This algorithm was applied to a yaw-reversal SACOM of $\psi_f = 30$ deg, with results presented in Sec. V; results for a pitch-reversal SACOM of $\theta_f = 80$ deg are presented in Sec. VI. The validity of these results is discussed in Sec. VII.

For agility comparison purposes, the importance of minimum-time maneuvers is obvious. The minimum-time solution, subject to appropriate constraints, is open loop and thus avoids pilot variability. Also, it turns out that all seven aerodynamic and TV controls are simultaneously engaged in a manner too fast and complicated to be executed by a human pilot. A number of works on minimum-time maneuvers employing TV controls were reported recently: minimum-time pitch-up,[12–14] roll,[15] and heading reversal[16] maneuvers, using simplified models. In our work, we compromised on exact optimality rather than on the model. To our knowledge ours is the first[17,18] to demonstrate the feasibility of a nearly pure yaw-reversal maneuver.

II. Attempts at Pure Pitch and Yaw Reversals

For a pitch maneuver in the vertical plane and symmetrical flight it is customary to consider longitudinal dynamics only. At high α, the asymmetrical forebody vortices may play havoc with this custom.

Figure 3 shows a simulated attempt at a pure pitch reversal using only pitch TV and the elevator. This is for an F-15B, using the following model. The open-loop nonoptimal pitch commands shown in Fig. 3a reflect amplitude and rate limitations. They are intended to provide maximum pitch acceleration and deceleration. Some of the responses are shown in Fig. 3b. There is a pitch reversal of 73 deg with (not shown) α up to 68 deg but also undesirable bank- and heading-angle motions of up to 70 and 30 deg, respectively. An animation of the maneuver is shown in Fig. 3c.

If the preceding pitch reversal is unacceptable, then the attempted pure yaw reversal using only yaw TV and rudder shown in Fig. 4a is outright disastrous, as seen in Figs. 4b and 4c. The yaw reversal is incomplete (with maximal α of 30 deg and β up to ± 20 deg; not shown), and the aircraft nearly rolls over.

These results show the need to employ a six-degree-of-freedom model. They motivate optimal control, where all aerodynamic and TV controls cooperate to produce the fastest orientation reversal while limiting undesired angular movements. They also show that the standard way of using test inputs for performance evaluation and comparison is not a good idea here; a better idea is to optimize performance. For agility, time is of course an appropriate optimization criterion.

III. Aircraft Model

A mathematical model for the six-degree-of-freedom dynamics of a twin-engine, thrust-vectored aircraft, the TV-equipped F-15B of our study, is presented next, with state vector $[\alpha, \beta, p, q, r, V, \psi, \theta, \varphi]$ and control vector $[\delta_a, \delta_e, \delta_r, \delta_{\Delta e}, \delta_z, \delta_y, \Delta\delta_z]$:

$$\dot{\alpha} = q + \{-[\bar{q}sC_x/MV - (g/V)\sin\theta + r\sin\beta]\sin\alpha$$
$$+ [\bar{q}sC_z/MV + (g/V)\cos\theta\cos\varphi - p\sin\beta]\cos\alpha\}\sec\beta \quad (1)$$

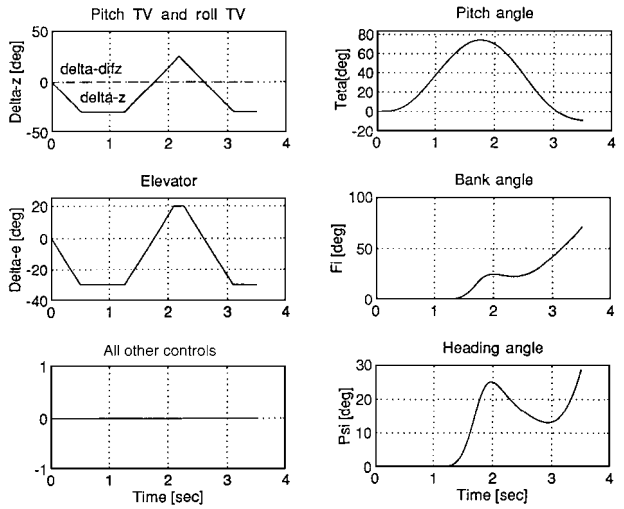

a) Controls b) Response

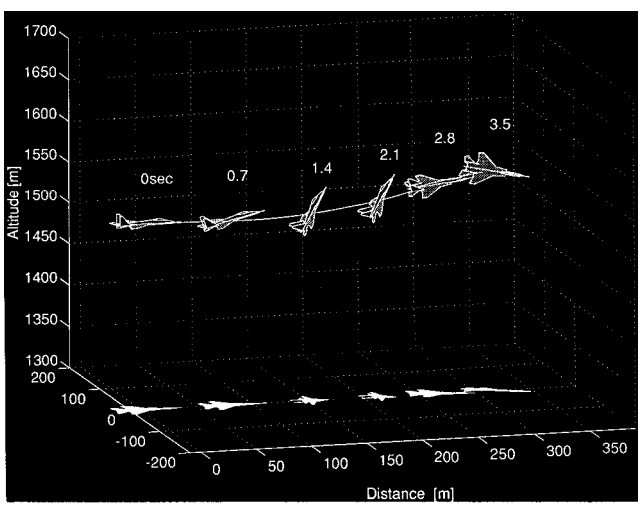

c) Three-dimensional view

Fig. 3 Attempt at a pure pitch-reversal SACOM.

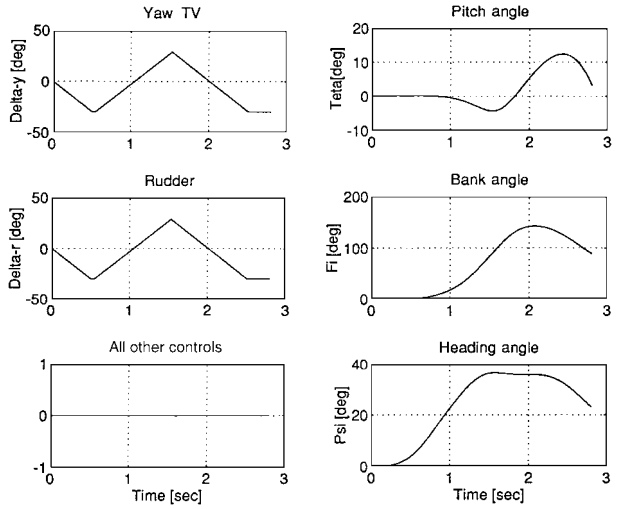

a) Controls b) Response

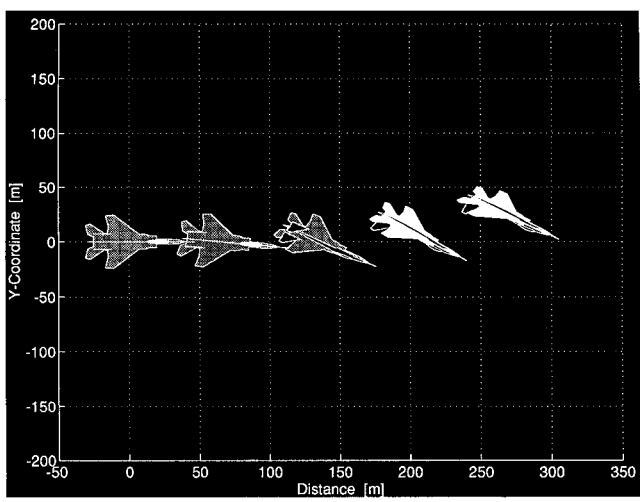

c) Top view

Fig. 4 Attempt at a pure yaw-reversal SACOM.

$$\dot{\beta} = -\{[\bar{q}sC_x/MV - (g/V)\sin\theta]\sin\beta + r\}\cos\alpha + [\bar{q}sC_y/MV + (g/V)\cos\theta\cos\varphi]\cos\beta - \{[\bar{q}sC_z/MV + (g/V)\cos\theta\cos\varphi]\sin\beta - p\}\sin\alpha \quad (2)$$

$$\dot{p} = \left\{-\left[(I_z - I_y)/I_x + I_{xz}^2/I_xI_z\right]qr + [1 - (I_y - I_x)/I_z]I_{xz}pq/I_x + \bar{q}sb/I_x(C_l + I_{xz}C_n/I_z)\right\}\Big/\left(1 - I_{xz}^2/I_xI_z\right) \quad (3)$$

$$\dot{q} = \bar{q}scC_m/I_y + [(I_z - I_x)/I_y]pr + I_{xz}(r^2 - p^2)/I_y \quad (4)$$

$$\dot{r} = \left\{\left[I_{xz}^2/I_xI_z - (I_z - I_x)/I_z\right]pq - [1 + (I_z - I_y)/I_x](I_{xz}/I_z)qr + (\bar{q}sb/I_z)[(I_{xz}/I_z)C_l + C_n]\right\}\Big/\left(1 - I_{xz}^2/I_xI_z\right) \quad (5)$$

$$\dot{V} = (\bar{q}sC_x/M - g\sin\theta)\cos\alpha\cos\beta + (\bar{q}sC_y/M + g\cos\theta\sin\varphi)\sin\beta + (\bar{q}sC_z/M + g\cos\theta\cos\varphi)\sin\alpha\cos\beta \quad (6)$$

$$\dot{\psi} = q\sin\varphi\sec\theta + r\cos\varphi\sec\theta \quad (7)$$

$$\dot{\theta} = q\cos\varphi - r\sin\varphi \quad (8)$$

$$\dot{\varphi} = p + r\cos\varphi\tan\theta + q\sin\varphi\tan\theta \quad (9)$$

$$C_x = C_L(\alpha, \delta_e)\sin\alpha - C_D(\alpha, \delta_e)\cos\alpha + T_x/\bar{q}s \quad (10)$$

$$C_y = C_{y0}(\alpha, \beta, \delta_e) + C_{y\delta_a}(\alpha)\delta_a + C_{y\delta_r}(\alpha)\delta_r + (b/2V)[C_{yr}(\alpha)r + C_{yp}(\alpha)p] + C_{y\beta^*}(\alpha, \beta) + C_{y\delta_{\Delta e}}(\alpha, \delta_e)\delta_{\Delta e} + T_y/\bar{q}s \quad (11)$$

$$C_z = -C_L(\alpha, \delta_e)\cos\alpha - C_D(\alpha, \delta_e)\sin\alpha + T_z/\bar{q}s \quad (12)$$

$$C_l = C_{l\beta}(\alpha, \beta)\beta + C_{l\delta_a}(\alpha, \delta_e)\delta_a + C_{l\delta_r}(\alpha, |\delta_r|)\delta_r + (b/2V)[C_{lp}(\alpha)p + C_{lr}(\alpha)r] + C_{l\delta_{\Delta e}}(\alpha, \delta_e)\delta_{\Delta e} + \Delta C_l(\alpha, \beta) + \left(T_{z_1} - T_{z_2}\right)l_y/\bar{q}sb \quad (13)$$

$$C_m = C_{m0}(\alpha, \delta_e) + (c/2V)C_{mq}(\alpha)q + \left(T_{z_1} + T_{z_2}\right)l_x/\bar{q}sc \quad (14)$$

$$C_n = C_{n\beta}(\alpha, \beta, \delta_e)\beta + C_{n\delta_a}(\alpha)\delta_a + C_{no}(\alpha, \beta) + C_{n\delta_r}(\alpha, \beta, \delta_r, \delta_e)\delta_r + (c/2V)[C_{np}(\alpha)p + C_{nr}(\alpha)r] + C_{n\delta_{\Delta e}}(\alpha, \delta_e)\delta_{\Delta e} + \Delta C_n(\alpha, \beta) + C_{n\beta^*}(\alpha, \beta) + \left[\left(T_{x_1} - T_{x_2}\right)l_y - \left(T_{y_1} + T_{y_2}\right)l_x\right]/\bar{q}sb \quad (15)$$

$$T_{x_{1,2}} = C_{fg}(\delta_z, \delta_y, N_{\text{pr}})T_i(M, h)B\cos\delta_y\cos\delta_{z_{1,2}}$$
$$T_x = T_{x_1} + T_{x_2} \quad (16)$$

$$T_{y_{1,2}} = C_{fg}(\delta_z, \delta_y, N_{\text{pr}}) T_i(M,h) B \sin\delta_y \cos\delta_{z_{1,2}} \tag{17}$$

$$T_y = T_{y1} + T_{y2}$$

$$T_{z_{1,2}} = -C_{fg}(\delta_z, \delta_y, N_{\text{pr}}) T_i(M,h) B \cos\delta_y \sin\delta_{z_{1,2}} \tag{18}$$

$$T_z = T_{z1} + T_{z2}$$

$$B = \frac{1}{\sqrt{\cos^2\delta_{z_{1,2}} + \cos^2\delta_y \sin^2\delta_{z_{1,2}}}} \tag{19}$$

$$\delta_z = \frac{\delta_{z1} + \delta_{z2}}{2}, \qquad \Delta\delta_z = \frac{\delta_{z1} - \delta_{z2}}{2}$$

Not shown are equations for Earth-axis velocity components needed to compute the aircraft position with respect to the ground. It is assumed that the mass and moments of inertia are constant. The throttle is at maximum dry position throughout the SACOM so as to provide maximum TV capability. Neglected are aeroelastic effects and the dependence of the thrust on an α and β (but not on altitude and Mach number).

The right-hand side of state equations (1–9) contains dimensionless coefficients C_i $(i = x, y, z, l, m, n)$ detailed in Eqs. (10–15). These contain the normalized forces (10–12) and normalized moments (13–15) produced by the aerodynamic controls and the normalized body-axis thrust components. The latter are additions to the usual equations and appear on the extreme right. The dependence of these thrust components on effective TV angles $(\delta_z, \delta_y, \Delta\delta_z)$ is given in Eqs. (16–19); here, the subscripts 1 and 2 refer to right and left jet engines, respectively.

Disturbances produced by the asymmetric forebody vortex at high α and β are characterized by the side-force coefficient $C_{y\beta^*}(\alpha, \beta)$ in Eq. (11) and by yawing moment coefficient $C_{n\beta^*}(\alpha, \beta)$ in Eq. (15); these produce unwanted banking and heading angles during a pitch-reversal SACOM. Because for high α $C_{n\beta^*}(\alpha, \beta = 0) \neq 0$, there is a lateral moment for a symmetrical flight. Unwanted roll motion during a yaw-reversal SACOM is due to the coupling terms $C_{l\beta}(\alpha, \beta)$, $C_{lr}(\alpha)$, and $\Delta C_l(\alpha, \beta)(\alpha)$ in Eq. (13).

Equations (1–19) are from Ref. 19, where their applicability is discussed. We used this particular model because of the availability to us of the needed numerical data. Note that the 29 coefficients in Eqs. (10–15) are nonlinear functions of state and control variables. They are represented as multidimensional polynomials of up to ninth order. These polynomials were data fitted[20] from empirical results and used by the U.S. Air Force; they are applicable for $-20 \leq \alpha \leq 90$ deg and $|\beta| \leq 30$ deg. The maneuvers are at low Mach number ($M < 0.3$), and hence the dependence of these coefficients on M is neglected, and incompressible flow is assumed. For simplicity, and with an error smaller than 5%, the magnitude of the thrust is assumed not to be affected by the TV [$C_{fg} = 1$ in Eqs. (16–18)].

The dynamics of the relatively fast actuators is neglected; however, limits on amplitudes and on rates of the controls are taken into account:

$$|\delta_a| \leq 20\,\text{deg}, \qquad |\delta_r| \leq 30\,\text{deg}, \qquad |\delta_y| \leq 30\,\text{deg}$$
$$|\delta_z| + |\Delta\delta_z| \leq 30\,\text{deg}, \qquad -30\,\text{deg} \leq \delta_e + \delta_{\Delta e} \leq 20\,\text{deg} \tag{20}$$
$$-30\,\text{deg} \leq \delta_e - \delta_{\Delta e} \leq 20\,\text{deg}$$

$$|\dot\delta_a| \leq 60\,\text{deg/s}, \qquad |\dot\delta_r| \leq 60\,\text{deg/s}, \qquad |\dot\delta_y| \leq 60\,\text{deg/s} \tag{21}$$
$$|\dot\delta_z| + |\Delta\dot\delta_z| \leq 60\,\text{deg/s}, \qquad |\dot\delta_e| + |\dot\delta_{\Delta e}| \leq 60\,\text{deg/s}$$

IV. Two-Stage Suboptimal Algorithm

We focus on the yaw-reversal SACOM; the pitch-reversal SACOM is entirely analogous. Let the aircraft equations (1–19) be written as

$$\dot x = f(x, \delta) \tag{22}$$

where the state x and control δ are

$$x^T = [\alpha, \beta, p, q, r, V, \psi, \theta, \varphi]$$
$$\delta^T = [\delta_e, \delta_a, \delta_r, \delta_{\Delta e}, \delta_z, \delta_y, \delta_{\Delta z}] \tag{23}$$

The optimal control problem is to find the optimal control $\delta^*(t)$ subject to the constraints

$$\delta_{\min} \leq \delta(t) \leq \delta_{\max}, \qquad \dot\delta_{\min} \leq \dot\delta(t) \leq \dot\delta_{\max} \tag{24}$$

subject to Eq. (22) and the state constraints

$$\theta_{\min} \leq \theta(t) \leq \theta_{\max}, \qquad \varphi_{\min} \leq \varphi(t) \leq \varphi_{\max} \tag{25}$$

and end conditions at $t = 0$, t_{f1}, and t_{f2}:

$$x^T(0) = (0, 0, 0, 0, 0, V_o, 0, 0, 0) \tag{26}$$

$$\psi(t_{f1}) = 30\,\text{deg}, \quad \dot\psi(t_{f1}) = 0, \text{ all other states at } t = t_{f1} \text{ are free} \tag{27}$$

$$\psi(t_{f2}) = 0, \quad \dot\psi(t_{f2}) = 0, \text{ all other states at } t = t_{f2} \text{ are free} \tag{28}$$

such that t_{f2} is minimum. To conform to the standard optimal control problem formulation, the state is to be augmented by the control variables

$$\bar x^T = [x^T, \delta^T]$$

so that $\dot\delta$ becomes the (constrained) control. Also, $\dot\psi(t_f) = 0$ is to be considered a terminal manifold given by Eq. (7).

This is a multipoint optimal control problem with state constraints, which in view of the complexity of Eq. (22) is extremely

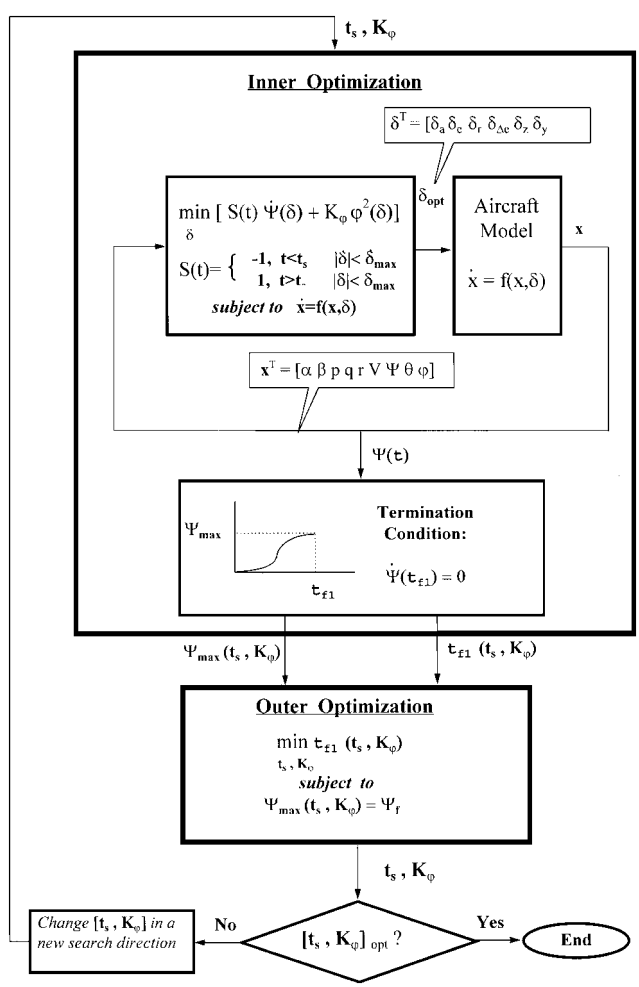

Fig. 5 Two-stage suboptimal algorithm for the to-target part of a yaw-reversal SACOM.

difficult. The first simplification is to break the problem into two: minimum time t_{f_1} to target and minimum recovery time $t_{f_2} - t_{f_1}$. Note that these are not identical problems because the initial conditions for the recovery phase are not the same as those for the to-target phase. Besides a probably negligible numerical consequence, this is a breakup into two problems with their own validity and usefulness. The second simplification is, instead of the state constraints (25), to consider a weighted criterion of time and square errors:

$$I = \int_0^{t_{f_1}} \left[1 + K_\theta \theta^2(t) + K_\varphi \varphi^2(t)\right] \mathrm{d}t \tag{29}$$

and likewise for the interval $[t_{f_1}, t_{f_2}]$. This makes sense because, as we have no idea of the reachability and controllability regions, we do not know what reasonable constraints one may impose on $\theta(t)$ and $\varphi(t)$. The performance index (29), on the other hand, allows for tradeoffs to be explored.

A further minor simplification is afforded by the observation, supported by simulations, that it is the roll motion that causes the undesirable pitching moment. Thus, by controlling roll we control pitch; consequently, in Eq. (29) K_θ can be taken as $K_\theta = 0$.

Because the problem is still too formidable, we resorted to a suboptimal solution based on intuitive physical reasoning. To achieve the fastest reorientation, the rate of turn should be as large as possible up to a last-minute switch time, beyond which it should slow maximally to arrive at the desired reorientation with zero rate. We thus make the following assumption.

Consider a reorientation maneuver of, e.g., the heading angle ψ from $\psi(0) = \dot{\psi}(0) = 0$ to $\psi(t_f) = \psi_f, \dot{\psi}(t_f) = 0$, while keeping undesired pitch and roll motions in check. To achieve this in minimum time t_f, we assume that the constrained controls δ should strive to maximize the weighted rate, $\dot{\psi} + K_\varphi \varphi^2$, on $[0, t_s]$ up to a switch time t_s and minimize it on $[t_s, t_f]$ so as to satisfy $\dot{\psi}(t_f) = 0$.

Although this working assumption appears plausible, there is of course no assurance that it holds in the optimal solution: for the nonlinear case, some time-optimal solutions are known to be counterintuitive.

The resulting two-stage suboptimal algorithm is shown in Fig. 5 for a to-target yaw maneuver. The input to the inner optimization stage are the switch time t_s and the weight K_φ. Note that, by definition of $S(t)$, $\dot{\psi}(t)$ is maximized for $t < t_s$ and minimized for $t > t_s$. For compactness of notation, the operations shown in Fig. 5 are in continuous time while executed, of course, in discrete time. Likewise, the dependence of $\dot{\psi}$ and φ on δ is not instantaneous as depicted in Fig. 5 but dynamic via the discretized model. The model (1–19), written as Eq. (22), is replaced by

$$\dot{x}_{k+1} = f(x_k, \delta_k), \qquad x_{k+1} = x_k + \dot{x}_{k+1} \Delta t_k \tag{30}$$

Having x_k at t_k and choosing δ_k, $\dot{\psi}_{k+2}$ and φ_{k+2} can be computed and

$$\min_{\delta_k} \left[S_{k+2} \dot{\psi}_{k+2}(\delta_k) + \varphi^2_{k+2}(\delta_k)\right] \tag{31}$$

is then executed by a gradient procedure to produce δ_k^{opt}; x_{k+1}^{opt} is computed by Eq. (30), and the process is continued over the next time interval where the gradient optimization is started with $\delta_{k+1} = \delta_k^{\mathrm{opt}}$.

The output of the inner optimization stage is the time t_{f_1} at which $\dot{\psi}(t_{f_1}) = 0$ and $\psi(t_{f_1}) = \psi_{\max}$. It is then up to the outer optimization

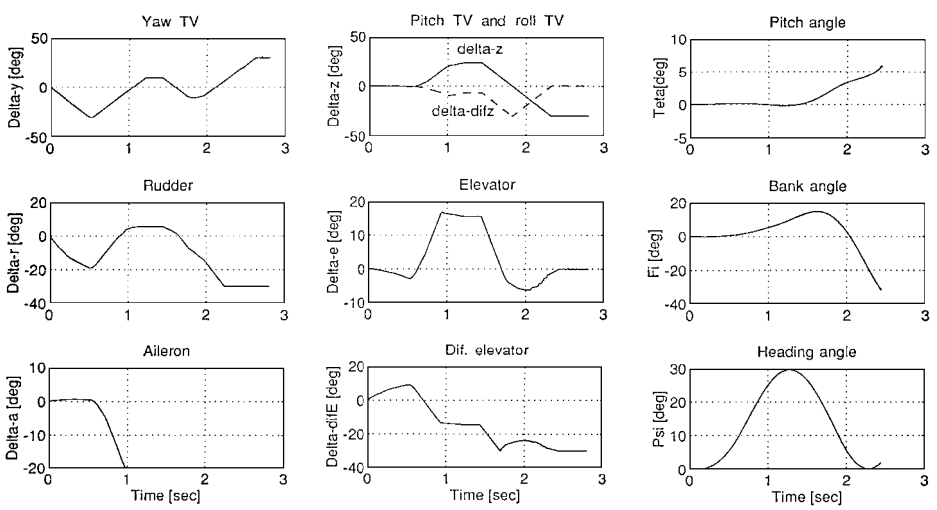

a) Controls **b) Response**

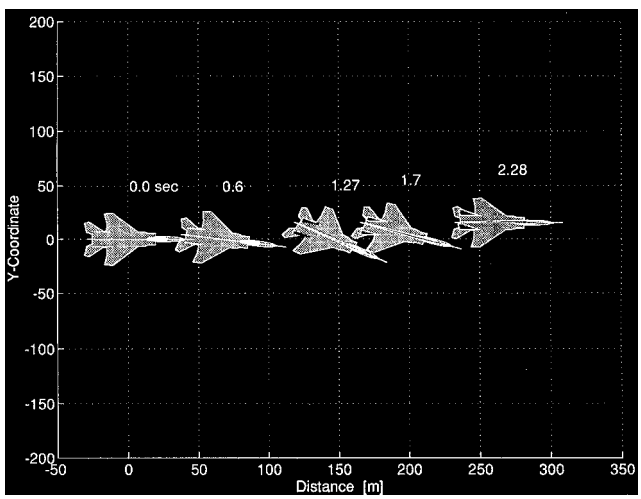

c) Top view

Fig. 6 Thirty-degree yaw-reversal SACOM.

stage to minimize t_{f_1} and to match $\psi_{\max}$ with $\psi(t_{f_1}) = 30$ deg; the minimization is over the switch time t_s and the weight K_φ. That K_φ was included in the outer optimization is an unusual and interesting feature, which requires an explanation. At first sight, a more or less monotonic tradeoff between minimum t_{f_1} and the $\varphi^2(t)$, error can be expected. This is true up to a value of K_φ, below which the increased drag due to increased errors in φ and θ starts to increase the minimum t_{f_1}. Thus, a time-optimal K_φ exists. For a fixed K_φ, the outer optimization is reduced to adjusting t_s so as to satisfy $\psi_{\max} = \psi_f$.

The algorithms for recovery of $\psi(t)$ to $\psi(t_{f_2}) = 0$ and for the pitch-reversal SACOM are entirely analogous.

The parametric two-stage optimization algorithm described earlier is much easier to set up and to apply than the maximum principle. Although it is ad hoc for the SACOM problem on hand, it can be generalized[17] and applied to similar problems. Indeed, to verify the algorithm against a known time-optimal solution, it is applied,[17] with very good results, to a spacecraft reorientation problem.

V. Results for a 30-Degree Yaw-Reversal SACOM

A to-target heading angle of 30 deg was chosen because the equations of motion are applicable only for $|\beta| \leq 30$ deg.

Three cases of the weighting coefficient K_φ are shown in Table 1. The indices 1 and 2 refer to the to-target and recovery phases, respectively. Whereas in cases 1 and 2 K_φ is a priori fixed, in case 3 $K_{\varphi 1}$ and $K_{\varphi 2}$ are time optimal. We see in case 1 that for low K_φ not only are the errors unacceptable, but also, as observed in the preceding section, the minimum times t_{f_1} and t_{f_2} are not the lowest. We note in case 2 that a purer SACOM is possible at the expense of the minimal time: a comparison of case 2 with case 3 shows a 13% increase of t_{f_2} as against a 32% decrease of maximal roll deviation and a 75% decrease of maximal pitch deviation.

Results for case 3 are shown in Fig. 6: the optimal controls in Fig. 6a, the angular responses in Fig. 6b, and a top view of the maneuver in Fig. 6c, where the final bank angle error of 32 deg can be discerned. Other variables were deliberately not controlled so as to monitor their response. Thus, the maneuver is accompanied

Table 1 Results for yaw-reversal SACOM for different K_φ

No.	Optimization parameters				Time to target t_{f_1}, s	Time to target and recovery t_{f_2}, s	Undesired aircraft deviations	
	$K_{\varphi 1}$	$K_{\varphi 2}$	t_{s1}, s	t_{s2}, s			$\lvert\varphi\rvert_{\max}$, deg	$\lvert\theta\rvert_{\max}$, deg
1	0	0	0.49	1.58	1.47	2.67	342	21
2	100	100	0.54	1.54	1.45	2.56	20	1.5
3	52	37	0.56	1.43	1.32	2.26	32	6

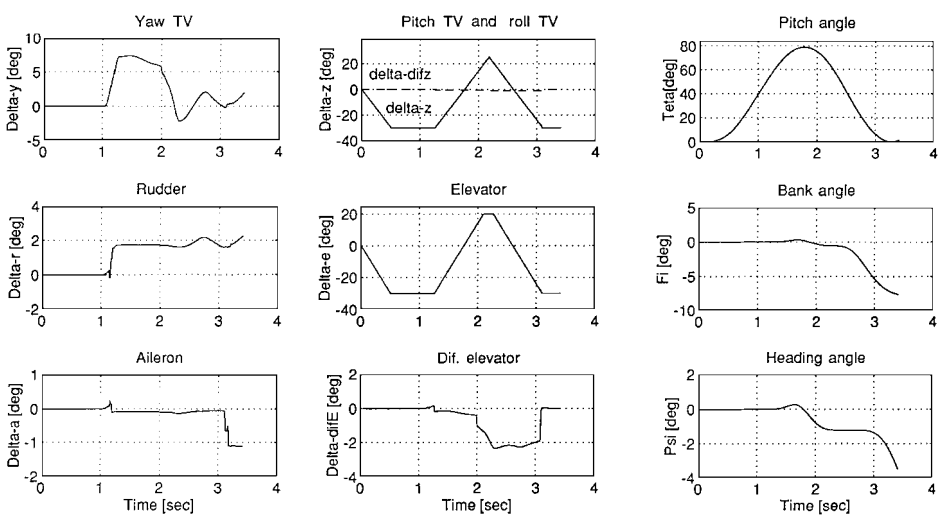

a) Controls **b) Response**

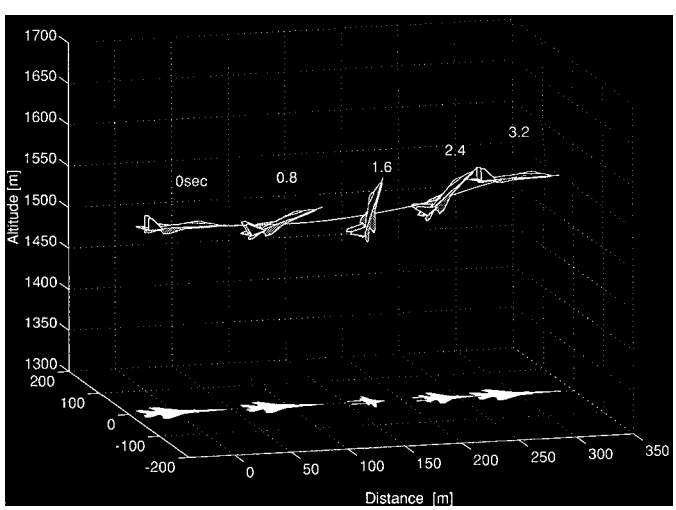

c) Three-dimensional view

Fig. 7 Eighty-degree pitch-reversal SACOM.

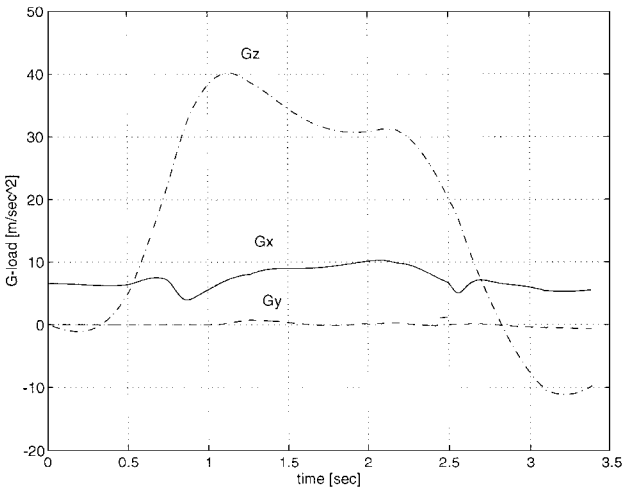

Fig. 8 The *g* loads during the pitch-reversal SACOM.

by a lateral displacement of 17 m, an 11-m drop in altitude from initial 1524 m, a 10-m/s increase in velocity from 110 m/s, and maximal α and β of 9 and -27 deg, respectively. The maximal g load is the lateral one of 14 m/s^2 at 1.5 s; the normal g load is only 8 m/s^2. Note that in the problem formulation it is the final heading rate $\dot{\psi}(t_2)$ that is to be zero. The roll, pitch, and yaw rates, however, were not constrained to be zero at t_{f_2}; they are -60, 0, and 23 deg/s, respectively.

VI. Results of an 80-Degree Pitch-Reversal SACOM

A to-target pitch angle of 80 deg was chosen to avoid numerical difficulties in the vicinity of the singular 90 deg; the equations of motion are applicable to $\alpha = 90$ deg.

In the algorithm described in Sec. IV for yaw, the pitch angle θ now replaces ψ. The weighting is now $K_\psi \psi^2$ on the heading error $\psi(t)$ only because limiting $|\psi(t)|$ tends to limit the roll error $|\varphi(t)|$.

In the first phase (to-target), θ deg $(t_{f_1}) = 80$ deg was achieved in 1.81 s, and in the second phase (recovery), θ deg (t_{f_2}) was completed at $t_{f_2} = 3.38$ s. The weight K_ψ was $K_{\psi 1} = 10^4$ and $K_{\psi 2} = 340$. The optimal $K_{\psi 1}$ is at the limit imposed by numerical considerations.

The results are shown in Fig. 7. It is seen that the pitch-reversal SACOM is much closer than the yaw-reversal SACOM to being pure. Also, the pitch TV and elevator are practically bang bang (considering rate constraints), in contrast to the yaw-reversal case. The maneuver is accompanied by a lateral displacement of 1 m, a 40-m rise in altitude from 1524 m, a 30-m/s drop in velocity from 110 m/s, and maximal α and β of 70 and 5 deg, respectively. The roll, pitch, and yaw rates at t_{f_2} are -3, 20, and -6.4 deg/s, respectively. The g loads are shown in Fig. 8. The normal g load is below the critical 5-g value and is of short duration.

VII. Conclusions

We demonstrate that, to help suppress adverse asymmetric side forces and moments at high-α and high-β values, one should consider a six-degree-of-freedom aircraft model and simultaneously employ all thrust vectoring and aerodynamic controls. For high-α values, this is true even for a pitch maneuver, where customarily only longitudinal dynamics are used.

A novel two-stage parametric optimization algorithm was developed; it was used to provide suboptimal solutions to minimum-time 30-deg yaw and 80-deg pitch reversals, using full, i.e., pitch, roll, and yaw, thrust vectoring. Surprisingly, the square-error weight, which usually is the chosen tradeoff parameter, was here subject to optimization.

The suboptimal algorithm produced instructive results. But how close are they to optimum? In particular, does our basic assumption on maximum switched angular rates hold? How close are our control time histories to the optimal ones? As in all suboptimal solutions, one never knows unless the optimal solution is available.

There are, needless to say, many other optimal maneuvers of TV-equipped fighter aircraft to be investigated. Our current research is being increasingly focused on the application of the TV technology to civil jet transports, where substantial safety benefits are feasible.

References

[1]Gal-Or, B., *Vectored Propulsion, Super-Maneuverability and Robot Aircraft*, Springer–Verlag, New York, 1991, pp. 56–78.

[2]Gal-Or, B., "Thrust Vectoring New Technology," *International Journal of Turbo and Jet Engines*, Vol. 11, No. 2, 1994, pp. 1–21.

[3]Gal-Or, B., "Thrust Vector Control Eyed for Passenger Aircraft: A Novel Methodology to Combine Jet-Engine Tests with Sub-Scale Proof-of-Concept Flight Tests," *International Journal of Turbo and Jet Engines*, Vol. 12, No. 4, 1995, pp. 241–251.

[4]Scott, W. B., "X-31 Kill Ratios Exceed Predictions," *Aviation Week and Space Technology*, Aug. 8, 1994, pp. 54, 55.

[5]Gal-Or, B., "Tailless Vectored Fighters," Flight Dynamics Directorate, USAF/AFOSR 89-0445, Wright–Patterson AFB, OH, July 1991.

[6]Gal-Or, B., "Safe Jet Aircraft," *International Journal of Turbo and Jet Engines*, Vol. 11, Nos. 1/2, 1994, pp. 1–9.

[7]Gal-Or, B., Sherbaum, V., and Lichtsinder, M., "Fundamentals of Catastrophic Failure Prevention by Thrust Vectoring," *Journal of Aircraft*, Vol. 32, No. 3, 1995, pp. 577–582.

[8]Qian, L., "Catastrophic Failure Prevention in Civil Transport Aircraft by Addition of Thrust Vectoring," M.S. Thesis, Dept. of Electrical Engineering, Technion—Israel Inst. of Technology, Haifa, Israel, June 1996.

[9]"Israel's Flight Test Jet-Powered RPV Fitted with Thrust-Vectoring Nozzles," *Aviation Week and Space Technology*, May 18, 1987, p. 21.

[10]Gal-Or, B., "Maximizing Thrust-Vectoring Control Power and Agility Metrics," *Journal of Aircraft*, Vol. 29, No. 4, 1992, pp. 647–651.

[11]Gal-Or, B., "Proposed Flight Testing Standards for Engine Thrust Vectoring to Maximize Kill Ratios, Poststall Agility and Flight Safety," *International Journal of Turbo and Jet Engines*, Vol. 12, No. 4, 1995, pp. 252–268.

[12]Mohler, R. R., "Nonlinear Control of High Performance Aircraft," *Proceedings of the 1993 American Control Conference* (San Francisco, CA), Vol. 2, 1993, pp. 1395–1398.

[13]Stalford, H., and Hoffman, E., "Thrust Vectoring Effect on Time-Optimal 90 Degree Angle of Attack Pitch-Up Maneuvers of a High Alpha Fighter Aircraft," *Proceedings of the AIAA Guidance, Navigation, and Control Conference*, AIAA, Washington, DC, 1989, pp. 840–846.

[14]Stalford, H., and Hoffman, E., "Maximum Principle Solutions for Time-Optimal Half-Loop Maneuvers of a High Alpha Fighter Aircraft," *Proceedings of the 1989 American Control Conference* (Pittsburgh, PA), Vol. 3, 1989, pp. 2453–2458.

[15]Bocvarov, S., Lutze, F. H., and Cliff, E. M., "Time-Optimal Reorientation Maneuvers for a Combat Aircraft," *Journal of Guidance, Control, and Dynamics*, Vol. 16, No. 2, 1993, pp. 232–240.

[16]Bocvarov, S., Cliff, E. M., and Lutze, F. H., "Aircraft Time-Optimal Reversal Maneuvers," *Proceedings of the AIAA Guidance, Navigation, and Control Conference*, AIAA, Washington, DC, 1994, pp. 146–153.

[17]Lichtsinder, A., "Sub-Optimal Control of Thrust-Vectored Aircraft Maneuvers," M.S. Thesis, Dept. of Electrical Engineering, Technion—Israel Inst. of Technology, Haifa, Israel, March 1995.

[18]Lichtsinder, A., Kreindler, E., and Gal-Or, B., "Thrust-Vectored Aircraft: Sub-Optimal Maneuvers," *Proceedings of the 35th Israel Annual Conference on Aerospace Sciences*, Technion, Haifa, Israel, 1995, pp. 150–156.

[19]Gal-Or, B., and Baumann, D., "Mathematical Phenomenology for Thrust-Vectoring-Induced Agility Comparisons," *Journal of Aircraft*, Vol. 30, No. 2, 1993, pp. 248–254.

[20]Baumann, D., "F15B High-Angle-of-Attack Phenomena and Spin Prediction Using Bifurcation Analysis," M.S. Thesis, U.S. Air Force Inst. of Technology, Wright–Patterson AFB, OH, Dec. 1989.